HIGH-VOLTAGE, HIGH-POWER, ZVS FULL-BRIDGE PWM CONVERTER EMPLOYING AN ACTIVE SNUBBER

J.A. Sabaté, V. Vlatkovic, R.B. Ridley, and F.C. Lee

Virginia Power Electronics Center
The Bradley Department of Electrical Engineering
Virginia Polytechnic Institute and State University
Blacksburg, Virginia 24061
Phone # (703) 231-4536

Abstract

The paper presents analysis, design, and application of a high-voltage, high-power, zero-voltage switched, full-bridge PWM converter with an active snubber in the secondary circuit. The nondissipative snubber completely eliminates the voltage overshoot and ringing across the rectifiers.

1. Introduction

The research and application of zero-voltage switching (ZVS) for the class of PWM converters is gaining increasing attention, as this converter family promises to combine the simplicity of PWM converters with the soft switching characteristics of resonant converters. A member of this family that is most widely used, especially in high-power and high-voltage applications, is the ZVS full-bridge (FB) PWM (ZVS-FB-PWM) converter [1-5]. This converter is controlled by the phase-shifted PWM technique which enables the use of all parasitic elements in the bridge to provide ZVS conditions for the active switches.

This topology, however, does not provide any means of absorbing the parasitic capacitances of the rectifier diodes. The interaction of rectifier capacitances with the leakage inductance of the transformer causes severe voltage overshoot and ringing across the rectifiers. This problem is exacerbated by the necessity of a large leakage inductance for the power transformer, resulting in a reduced ringing frequency. This makes the use of RC snubber in the secondary impractical [5]. The problem is particularly severe in high-voltage, high-power applications, where the reverse recovery time of the rectifiers is excessive, because Schottky diodes cannot be used.

[1] The work was supported by the International Business Machines Co., Kingston, NY, and by the Virginia Center for Innovative Technology, Technology Development Center for Power Electronics.

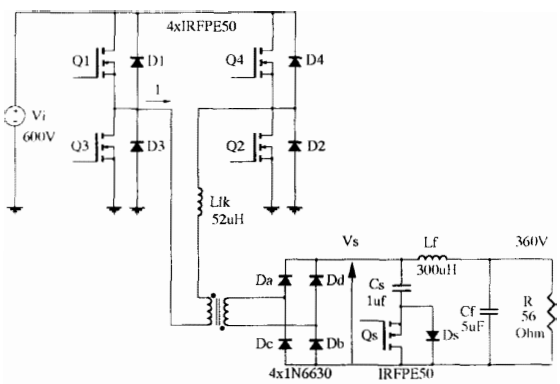

Fig. 1. : ZVS-FB-PWM converter with the active snubber.

Several solutions to this problem have been suggested. The simplest one [2] is to use a clamp circuit across the rectifiers. The clamp circuit limits the peak voltage in the secondary, but does nothing to damp or prevent the ringing. The excessive ringing causes EMI and control problems. The amount of power dissipation of the clamp circuit also makes it impractical for use in high-voltage, high-power applications above several hundred volts and several kilowatts.

Another attempt is to use a low-leakage power transformer with a separate inductor in the primary, and to clamp the voltage in the primary circuit [3,4]. This approach has two drawbacks. One is the requirement for an extra inductor, which increases the size and reduces the efficiency of the converter. The other is the high frequency ringing between the parasitic capacitance of the rectifiers and the leakage inductance, which may require the use of an RC snubber in the secondary.

This paper presents the analysis, design, and application of the ZVS-FB-PWM converter with an active snubber across the rectifiers. The snubber completely eliminates voltage overshoot and ringing in a nondissipative manner. These attributes make the snubber particularly useful in high-voltage, high-power applications.

2. Proposed Converter

The proposed converter is shown in Fig. 1. When the secondary voltage is high, the active snubber, (Q_s, D_s, C_s), connects a large capacitor in parallel with the rectifiers. The resonant frequency of the snubber capacitor and leakage inductance has to be small compared to the switching frequency, *i.e.* $2\pi\sqrt{n^2L_{lk}C_s} \gg T_s$, where T_s is the switching period. Consequently, the rectifier voltage is clamped to the steady-state value of the snubber capacitor voltage, and there is no voltage overshoot in the secondary.

In steady-state operation, the average current through the snubber capacitor is zero. The energy from the leakage inductance of the transformer charges the snubber capacitor through the snubber diode. The capacitor delivers this energy to the load through the snubber MOSFET.

The bridge is operated with phase-shift control in the same manner as in the conventional ZVS-FB-PWM converter [1,2,3,5]. Figure 2 shows the typical waveforms for the converter with the snubber circuit, the current through the snubber capacitor, and the driver signal of the snubber MOSFET. The converter operation for a half cycle is described as follows:

t_1 to t_2: In the primary, Q_4 and D_1 are conducting. In the secondary D_c and D_d are conducting. The primary current follows the output filter current.

t_2: Q_4 turns off, and the current through the primary charges the output capacitance of Q_4 and discharges the output capacitance of Q_2, turning on diode D_2.

t_2': Diode D_2 starts conducting, and immediately after that, Q_2 is turned on with zero voltage.

In the secondary, all four diodes start conducting, shorting the secondary of the transformer.

t_2 to t_3: The primary current circulates through diodes D_1 and D_2 until it reaches zero. The secondary of the transformer is shorted.

t_3 to t_4: Primary current circulates through Q_1 and Q_2. The secondary of the transformer is shorted.

t_4: The primary current reaches the reflected filter inductor current.

t_4 to t_5: The voltage in the secondary of the transformer starts increasing, and the leakage inductance of the transformer starts resonating with the rectifier diodes' capacitance.

t_5: The secondary voltage, V_s, reaches the snubber capacitor voltage, and the snubber diode starts conducting. The secondary is clamped to the value of the snubber capacitor voltage.

t_5 to t_6: The current through the snubber capacitor decreases until it reverses sign at t_6. At this time the snubber MOSFET has to be already turned on.

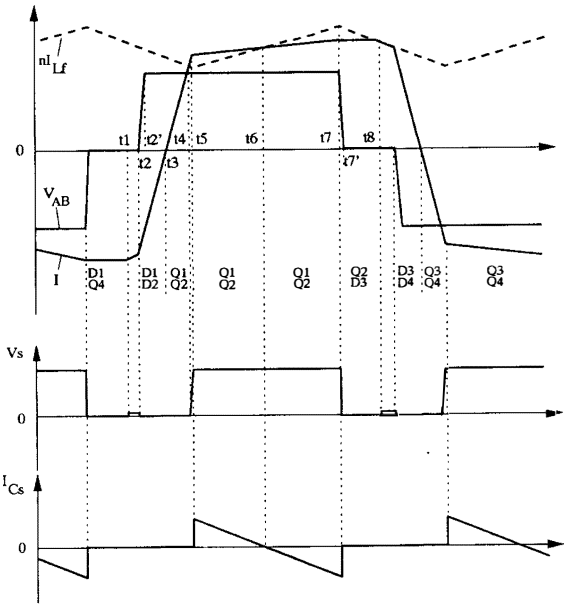

Fig. 2. : FB-ZVS-PWM converter and primary and secondary waveforms, snubber's current, and Q_s gate drive signal.

t_6: The snubber current naturally commutates from D_s to Q_s. For this reason D_s does not need to be a fast diode, and the body diode of Q_s is used.

t_6 to t_7: The current through the snubber capacitor flows through the MOSFET Q_s until Q_1 is turned off. The snubber MOSFET has to be turned off when the secondary voltage starts decreasing.

t_7: When the voltage in the secondary starts decreasing, the primary current is smaller than the reflected filter inductor current. Therefore, the output filter inductor current starts free-wheeling through the rectifiers. The secondary of the transformer is shorted.

The current in the leakage inductance, charges the output capacitance of Q_1 and discharges the capacitance of Q_3; the diode D_3 is subsequently turned on.

t_7': Diode D_3 starts conducting, and immediately after that, Q_3 is turned on with zero voltage.

t_7 to t_8: The primary current remains constant (assuming that the switches have zero on resistance and the diodes have zero forward drop). The secondary is still shorted.

t_8: The primary current reaches the reflected output filter inductor current. Rectifier diodes D_c and D_d stop conducting.

The most important changes in the converter operation due to the introduction of the snubber are:

RidleyBox®

Knowledge is Power

RIDLEY ENGINEERING
www.ridleyengineering.com

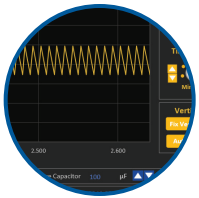

RidleyWorks® Lifetime License

- Power Stage Designer
- Power Stage Waveforms
- Magnetics Designer
- Transfer Function Bode Plots
- Closed Loop Design
- Automated FRA Control
- LTspice® Automated Link
- PSIM® Automated Link

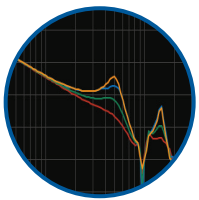

4-Channel Frequency Response Analyzer

- Frequency Range 1 Hz - 20 MHZ
- Source Control from 1 mV - 4 V P-P
- Built-In Injection Isolator
- Bandwidth 1 Hz - 1 kHz
- Automated Setup from RidleyWorks®
- Direct Data Flow into RidleyWorks®

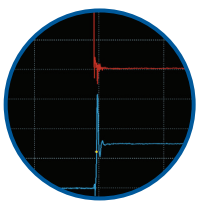

4-Channel 200 MHz Oscilloscope

- Picoscope® 5444D 4-Channel Oscilloscope
- 200 MHz Bandwidth
- 1 GS/s at 8-bit res; 62.5 MS/s at 16-bit res
- Signal Generator up to 20 MHZ
- Computer Controlled

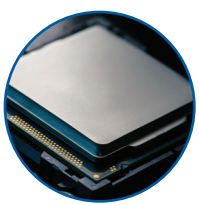

Embedded Computer

- Intel® Computer with 32 GB RAM, 256 GB SSD
- Intel® HD Graphics 620
- Integrated Dual Band Wireless, Bluetooth 4.2
- Dual HDMI and USB Ports, Ethernet

Differential Probes

Line Injector

Accessories

Output Impedance

Impedance Test Kit

- There is no ringing in the secondary voltage, reducing the voltage stress in the rectifiers and eliminating snubber losses.
- The transformer secondary current is the sum of the output filter inductor current and the current through the snubber capacitor.
- The peak primary current is reduced because the current through the snubber capacitor is negative when the output filter inductor current reaches its peak.
- The ZVS for Q_1 and Q_3 is achieved in exactly the same manner as for Q_2 and Q_4. The output filter inductor does not intervene in the process.

3. Analysis

Assuming that the snubber capacitor is chosen sufficiently large, the voltage in the secondary is a square wave with a peak value equal to the voltage across the snubber capacitor. Consequently, the output voltage, V_{out}, is determined by the duty cycle of the secondary voltage, D_{eff}, and the snubber capacitor voltage, V_{cs}, as:

$$V_{out} = D_{eff}\ V_{cs} \quad . \tag{1}$$

Previous analysis of the ZVS-FB-PWM converter [5] shows how to calculate the primary duty cycle, D, knowing the circuit parameters. That part of the analysis is also valid for this circuit. The goal of the analysis presented here is to determine the snubber capacitor voltage.

During the interval t_5 to t_7 the slope, S_{ls}, of the transformer secondary current is determined by:

$$S_{ls} = \frac{n\ V_{in} - V_{cs}}{n^2\ L_{lk}}, \tag{2}$$

where V_{in} is the input voltage, n is the transformer turns ratio ($n = N_S/N_P$), V_{cs} is the steady state voltage of the snubber capacitor, and L_{lk} is the leakage inductance of the transformer. The current through the snubber capacitor is the difference between the secondary current and the filter inductor current. The slope of the snubber capacitor current is:

$$S_{lcs} = \frac{n\ V_{in} - V_{cs}}{n^2\ L_{lk}} - \frac{V_{cs} - V_{out}}{L_f}, \tag{3}$$

where V_{out} is the output voltage and L_f is the value of the output filter inductor.

The difference between transformer secondary current and the filter inductor current at time , t_5, corresponds to the resonance between L_{lk} and the rectifiers capacitance when the secondary voltage reaches V_{cs}, plus the reverse recovery current through the rectifiers that are turned off. Assuming that the rectifiers capacitance is constant, this current difference, Δi_{sec}, can be calculated as [2]:

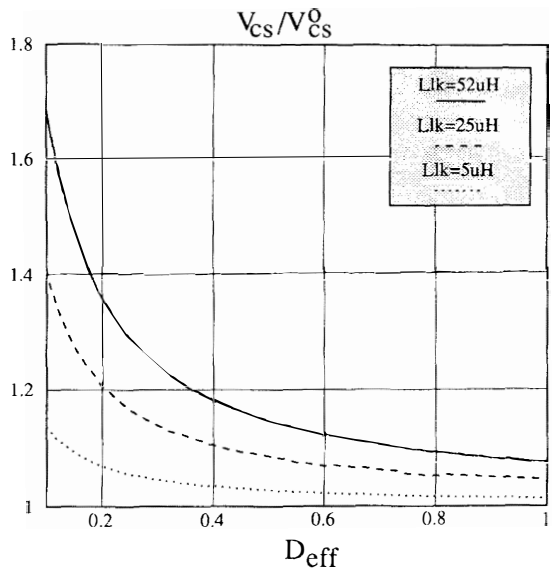

Fig. 3. : Ratio of V_{cs}/V_{cs}^{o} vs. secondary duty cycle: For leakage inductances 5 μH, 25 μH, and 50 μH.

$$\Delta i_{\text{sec}} = \frac{n\ V_{in}}{\sqrt{\frac{L_{lk}}{C_{\text{sec}}}}} \cos\left[\sin^{-1}\left(\frac{V_{cs} - n\ V_{in}}{n\ V_{in}}\right)\right] + 2\,|i_{rr}|, \tag{4}$$

where C_{sec} is the sum of rectifiers and transformer winding capacitances, and i_{rr} is the peak reverse current through one rectifier diode due to the reverse recovery.

Since the average current through the snubber capacitor is zero in steady state, the following implicit expression for the snubber capacitor voltage is obtained:

$$\left(\frac{V_{cs} - V_{out}}{L_f} + \frac{V_{cs} - n\ V_{in}}{n^2\ L_{lk}}\right) \frac{V_{out}\ T_s}{4\ V_{cs}} =$$

$$\frac{V_{in}\ n}{\sqrt{\frac{L_{lk}}{C_{\text{sec}}}}} \cos\left[\sin^{-1}\left(\frac{V_{cs} - n\ V_{in}}{n\ V_{in}}\right)\right] + 2\,|i_{rr}|, \tag{5}$$

where T_s is the switching period.

Using Eq. (1), Eq. (5) can be written as a function of the effective duty cycle:

$$\left[V_{cs}\left(\frac{1-D_{eff}}{L_f} + \frac{1}{n^2 L_{lk}} \right) - \frac{V_{in}}{n L_{lk}} \right] \frac{D_{eff} T_s}{4} =$$

$$= \frac{n V_{in}}{\sqrt{\frac{L_{lk}}{C_{sec}}}} \cos\left[\sin^{-1}\left(\frac{V_{cs}}{n V_{in}} - 1 \right) \right] + 2|i_{rr}|. \qquad (6)$$

This equation can be solved explicitly for V_{cs} (the solution is provided in the appendix).

To illustrate the variation of V_{cs} with respect to D_{eff}, V_{cs} is compared with the steady state secondary voltage in the ideal case, $C_{sec} = 0$, and $i_{rr} = 0$. In this ideal case , Eq. (6) gives:

$$V_{cs}^{o} = n V_{in} \frac{L_f}{L_f + (1 - D_{eff}) n^2 L_{lk}}. \qquad (7)$$

Figure 3 shows the ratio V_{cs}/V_{cs}^{o} as a function of D_{eff} for different values of L_{lk} and for the following circuit parameters:

- $|i_{rr}| = 0.6\,A$
- $C_{sec} = 130\,pF$
- $V_{in} = 600\,V$
- $L_f = 300\,\mu H$
- $n = 1$
- $T_s = 10\,\mu$ sec .

The graph in Fig. 3 shows several things that influence the design of the converter with the snubber. First, the steady-state secondary voltage with the snubber is always higher than the secondary voltage in the ideal case; the secondary voltage increases with an increase of L_{lk} and/or C_{sec}. Second, there is a sharp increase in V_{cs} as D_{eff} is small (less than 0.2). This operation area should be avoided, because of the increased voltage stress on the rectifier diodes.

Figure 3 does is not shown for values of duty cycle smaller than 0.05 because these duty cycles correspond to a time shorter than the time required for the secondary voltage to rise (*i.e.*, $D_{eff} = 0.05$, or $D_{eff} T_s = 0.25\,\mu sec.$) For these small duty cycles Eq. (6) is not valid. The rising time of the secondary voltage can be calculated from knowing the leakage inductance and the total capacitance in the secondary:

$$t_{rise} = \frac{\pi}{2} \sqrt{L_{lk} C_{sec}}, \qquad (8)$$

where t_{rise} corresponds to the time required for the secondary voltage to reach $n\,Vin$.

4. Experimental Realization

The breadboard used to test the presented active snubber concept and analysis has the following specifications (Fig. 1):

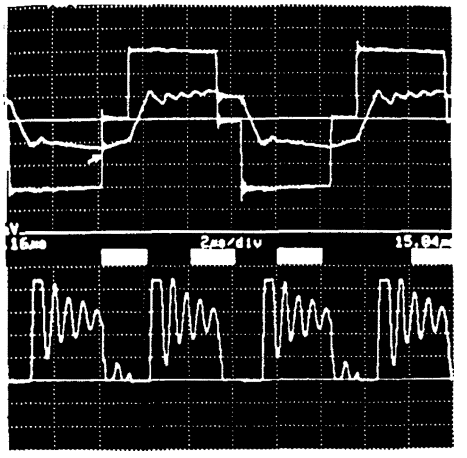

Fig. 4. : Without active snubber: Voltage and current in the primary (top waveforms) and voltage across the rectifier (lower waveform), full-load operation. (Scales: voltage: 200 V/div., current: 5 A/div., time: 2 μsec/div.)

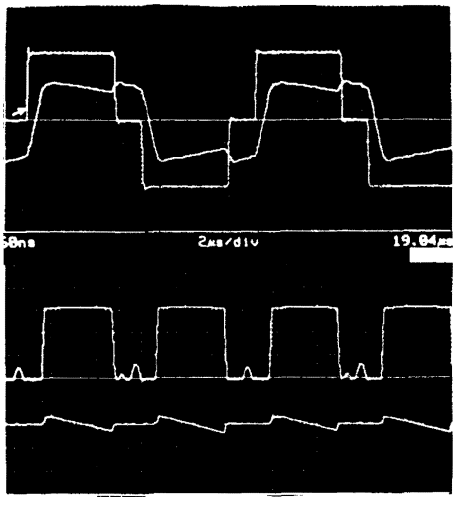

Fig. 5. : With active snubber Primary and secondary voltages (top waveforms) and primary and snubber currents (lower waveforms), full-load operation. (Scales: voltage: 200 V/div., current: 2 A/div., time: 1 μsec/div.)

- input voltage $V_{in} = 600\,V$
- output voltage $V_{out} = 360\,V$
- output Power $P_{out} = 2\,kW$
- switching frequency $f_s = 100\,kHz$

Ridley Labs

The Ultimate Education

REMOTE HANDS-ON WORKSHOPS

POWERDESIGNWORKSHOPS.COM

RIDLEY ENGINEERING
www.ridleyengineering.com

4-Day Design Workshops Learn how to design, build, test and measure faster and with more precision from the leader in power electronics design education since 1991.

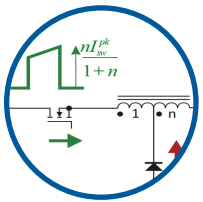

Choose a Topology
Learn about popular topologies used worldwide for modern applications.

Apply Basic Magnetics
Understand the single equation needed to begin design execution.

Apply Advanced Magnetics
Optimize magnetics losses and incorporate advanced analyses.

Model and Measure
Learn how to model non-linear circuits and measure the results.

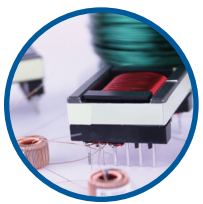

Voltage- and Current-mode Control
Measure the response and apply control and loop design techniques.

Design Transformers
Design, build and test transformers and inductors in a hands-on lab.

Design Snubber
Optimize a snubber in one pass using software and hardware applications.

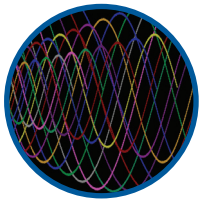

Measure Efficiency
Compete with fellow classmates to accurately measure efficiency.

Design GaN
Learn first-hand how to design with the latest GaN technologies for converters.

Design Synchronus Rectifiers
Become familiar with synchronous rectifiers and design applications.

Optimize Control
Intuitively and visually shape and adjust loops for optimal performance.

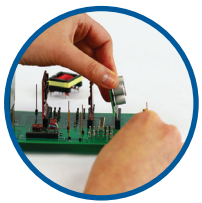

Prototype with SwitchBit®
Develop a working prototype for multiple applications in just a few hours.

- transformer turns ratio $n = 1$
- maximum primary duty cycle $D_{max} = 0.8$
- secondary duty cycle $D_{eff} = 0.6$
- transformer leakage inductance $L_{lk} = 52\,\mu H$
- rectifier's diodes capacitance $C_{sec} = 130\,pF$
- peak reverse recovery current $|i_{rr}| = 0.6\,A$.

Figure 4 shows the converter waveforms at full-load using the clamp circuit proposed in [2,5]. Figure 5 shows the corresponding waveforms at the same power level (2 kW) using the active snubber. The severe ringing seen in Fig. 5 is completely eliminated.

Figure 6 shows the converter waveforms at power level of 1 kW. The current through the snubber capacitor has not changed significantly. This supports the assumption that was used to derive Eq. (6).

The slope of the current when reverse voltage is applied to the diodes is limited by the leakage inductance. Consequently I_{rr} is relatively small and does not vary significantly with the load current. Therefore, the snubber capacitor voltage is almost independent of the converter load current.

Figure 7 shows the values of secondary voltage, V_{cs}, as a function of D_{eff} as predicted by Eq. (6) and the measurements of V_{cs}.

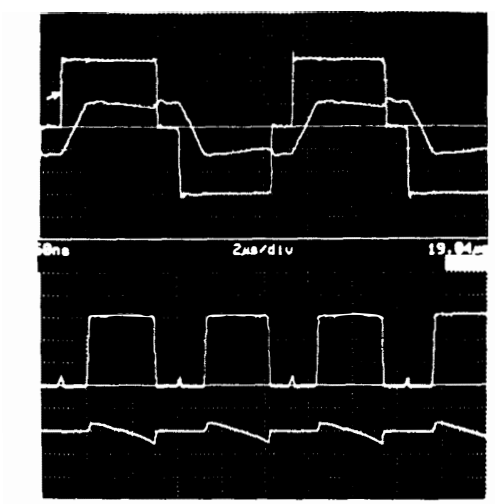

Fig. 6. : With active snubber at 50 % load Primary and secondary voltages (top waveforms) and primary and snubber currents (lower waveforms), full-load operation. (Scales: voltage: 200 V/div., current: 2 A/div., time: 1 μsec/div.)

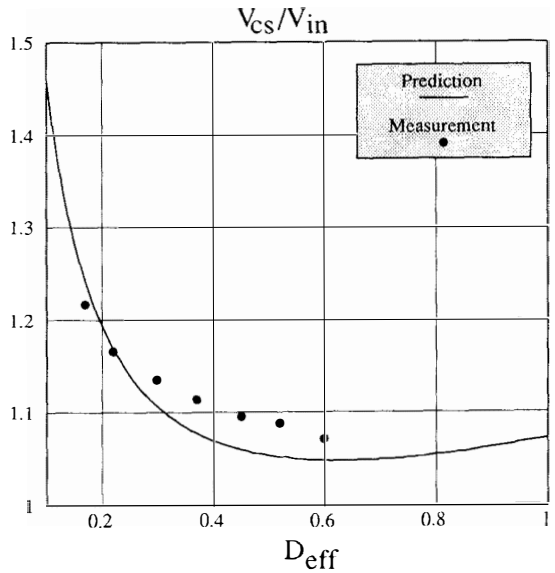

Fig. 7. : Snubber capacitor voltage vs. secondary duty cycle Calculated (solid line) and measured (dashed line).

4.1. Control of the snubber

The gate-drive signal for Q_s can be generated by sensing the secondary voltage of the power transformer and turning on Q_s whenever this voltage reaches V_{cs}. However, a simplified the gate drive is proposed without sensing the secondary voltage of the power transformer. Block diagram of this gate drive circuit is shown in Fig. 8.

Since the transformer secondary voltage is delayed ($t_2 - t_5$, Fig. 2), the switch Q_s has to be turned on with a delay , t_d, greater than the maximum delay of the secondary voltage. The maximum delay of the secondary voltage occurs at full-load low-line. Since in this case t_d is fixed, for proper circuit operation, t_d and ΔD_{eff} have to satisfy

$$\Delta D_{max} \le 2\,\frac{t_d}{T_s} \le \frac{D_{min}}{2}, \qquad (9)$$

where D_{min} is the primary duty cycle at minimum load, and D_{min} is defined as $\Delta D_{max} = D_{max} - D_{eff}$ (at full-load low-line).

5. Conclusions

The ringing between the leakage inductance of the transformer and the parasitic capacitance of the rectifier diodes represents the main obstacle for using the ZVS-FB-PWM converter in high-voltage, high-power applications. The ringing imposes a severe voltage stress on the

rectifier diodes, and calls for use of some kind of snubber circuit in the secondary. At high power and voltage levels, the energy of this ringing is so high that the use of any type of dissipative snubber becomes impractical.

The paper presents the solution to this problem. The proposed active snubber used in the secondary completely eliminates the ringing. This significantly reduces the voltage stress on the rectifiers, making possible the use of faster, lower voltage rectifier diodes.

The ringing of the parasitic capacitance of the rectifiers and the leakage inductance of the transformer is eliminated in a nondissipative manner, thus increasing the overall efficiency of the circuit. The active snubber employs only a high-voltage low-power MOSFET and a high-voltage capacitor. The control of the snubber switch is simple and utilizes the PWM signal controlling the primary switches with a time delay.

The paper also presents the complete steady-state analysis of the ZVS-FB-PWM converter employing the active snubber. The analysis shows that the transformer secondary voltage is a function of the steady-state duty cycle, and gives the equation to calculate the steady-state secondary voltage. The breadboard built shows the validity of the proposed solution. The results of the analysis are in good agreement with the experimental results.

6. References

[1] Z.D. Fang, D.Y. Chen, and F.C. Lee, "Designing a High Frequency Snubberless FET Power Inverter," *Proc. of POWERCON 11*, D1-4 pp. 1-10, 1984.

[2] L.H. Mweene, C.A. Wright, and M.F. Schlecht, "A 1 KW, 500 KHz Front-End Converter for a Distributed Power Supply System," *IEEE APEC'89 Proc.*, pp. 423-432, 1989.

[3] R. Redl, N.O. Sokal, and L. Balogh "A Novel Soft-Switching Full-Bridge DC/DC Converter: Analysis, Design Considerations, and Experimental Results at 1.5 kW, 100 kHz," *IEEE Power Electronics Specialists' Conf. Rec.*, pp. 162-172, 1990.

[4] V. G. Agelidis, P. D. Ziogas, and G. Joos "An Efficient High Frequency High Power Off-Line DC-DC Converter Topology," *IEEE Power Electronics Specialists' Conf. Rec.*, pp. 173-180, 1990.

[5] J.A. Sabaté, V. Vlatkovic, R.B. Ridley, F.C. Lee and B.H.Cho, "Design Considerations for High-Voltage, High-Power, Full-Bridge, Zero-Voltage-Switched PWM Converter," *IEEE APEC'90 Proc.*, pp. 275-284, 1990.

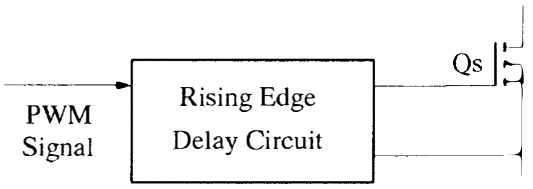

Fig. 8. : Block diagram of the snubber MOSFET gate drive.

[6] K. Harada and H. Sakamoto, "Switched Snubber for High Frequency Switching," *IEEE Power Electronics Specialists' Conf. Rec.*, pp. 181-188, 1990.

Appendix

An explicit expression for the voltage V_{cs} can be obtained from Eq. (6) as follows:
Using

$$\cos\left[\sin^{-1}\left(\frac{V_{cs}-n\,V_{in}}{n\,V_{in}}\right)\right]=\sqrt{1-\left(\frac{V_{cs}-V_{in}}{n\,V_{in}}\right)^2} \qquad (A.1)$$

in Eq. (6), and solving for V_{cs},

$$V_{cs}=X+\sqrt{X^2-Y}\,, \qquad (A.2)$$

where

$$X=E\,n\,V_{in}+F\,|i_{rr}| \qquad (A.3)$$

$$Y=G\,n\,V_{in}^2-H\,|i_{rr}|^2-\Phi\,n\,V_{in}\,|i_{rr}| \qquad (A.4)$$

$$E=A\,B+\Phi\,\frac{1}{Z_o^2} \qquad (A.5)$$

$$F=\Phi\,A \qquad (A.6)$$

$$G=\Phi\,B^2 \qquad (A.7)$$

$$H=2\,F \qquad (A.8)$$

with:

$$Z_o=\sqrt{\frac{n^2\,L_{lk}}{C_{\sec}}} \qquad (A.9)$$

$$A=\frac{D_{eff}\,T_s}{4}\left(\frac{1}{n^2\,L_{lk}}-\frac{1-D_{eff}}{L_f}\right) \qquad (A.10)$$

$$B=\frac{D_{eff}\,T_s}{4\,n^2\,L_{lk}} \qquad (A.11)$$

$$\Phi=\frac{1}{A^2+\frac{1}{Z_o^2}}\,. \qquad (A.12)$$

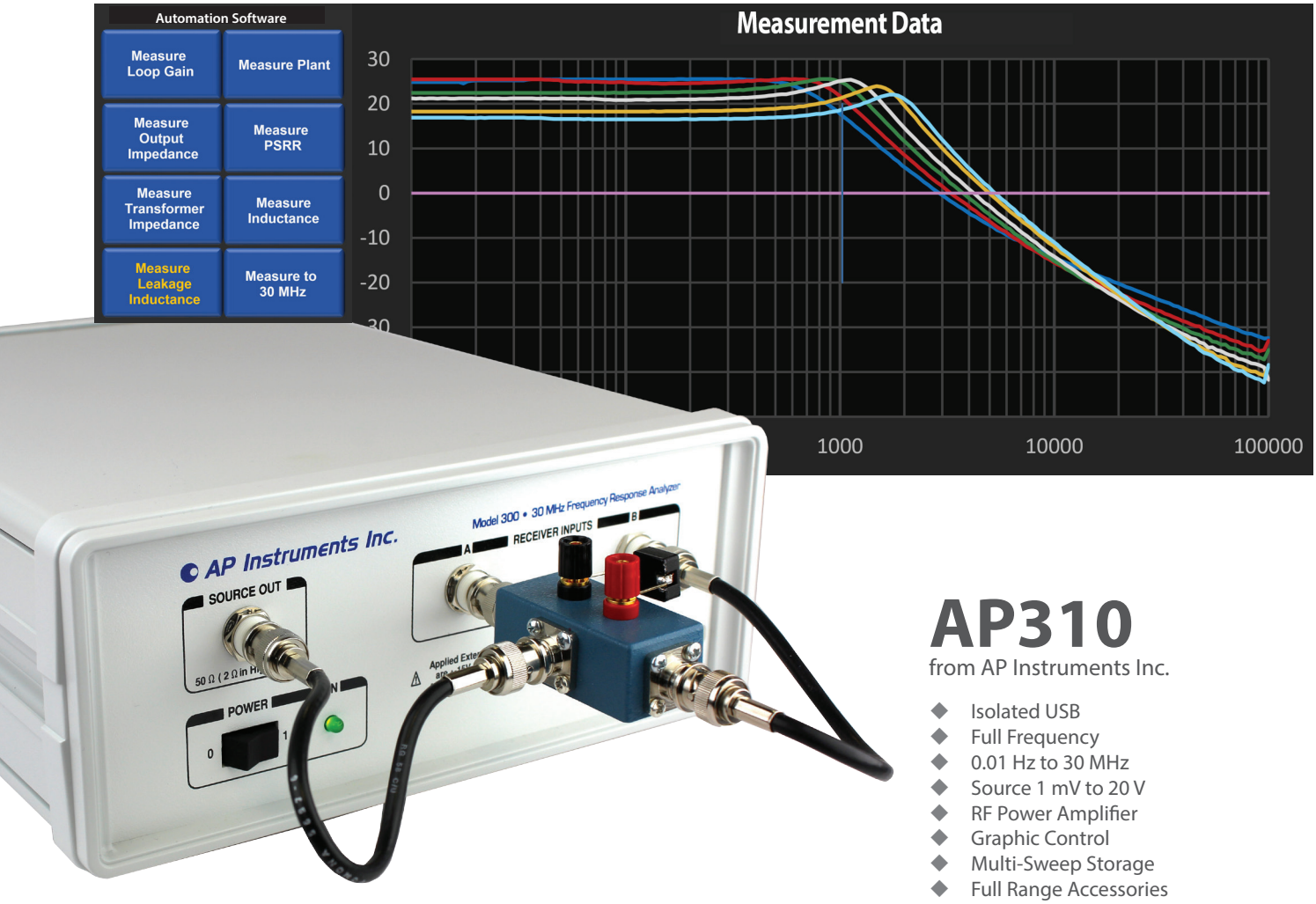

AP310

from AP Instruments Inc.

- Isolated USB
- Full Frequency
- 0.01 Hz to 30 MHz
- Source 1 mV to 20 V
- RF Power Amplifier
- Graphic Control
- Multi-Sweep Storage
- Full Range Accessories
- Maximum Productivity
- Fully-Automated Loop Design
- Support from Industry Experts
- Easy to Use
- One-Button Setup

AP310 is the industry's only full-featured frequency response analyzer designed specifically for power supplies. Enhance the experience with RidleyWorks® software for seamless integration between power supply design and measurement. *Made in California since 1995.*

RIDLEYENGINEERING.COM

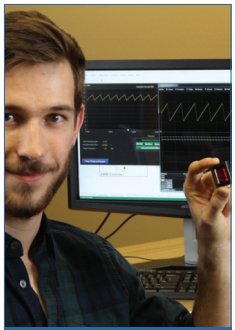

Workshops

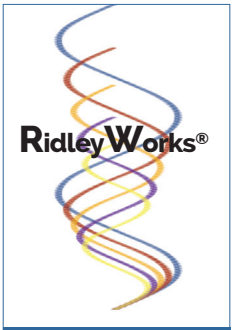

Design Software

Analyzer

Design Ideas

RIDLEY ENGINEERING

601 E Daily Drive, Suite 112 | Camarillo CA 93010 | info@ridleyengineering.com | +1 805 504 2212 | POWER SUPPLY DESIGN CENTER GROUP on FaceBook

Full Range Measurements

0.01Hz Minimum frequency
for PFC measurement
30 MHz Maximum frequency
for full magnetics characterisation
117 dB Dynamic range
Exceptional performance
for high-noise environments,
challenging impedance and PSRR

Power Amplifier Output

1 mV Minimum source value
for sensitive systems
20 V p-p Source for high-power
and high-drive systems
2 Ohm Output impedance
500 mA Current capability
Self protected from damage

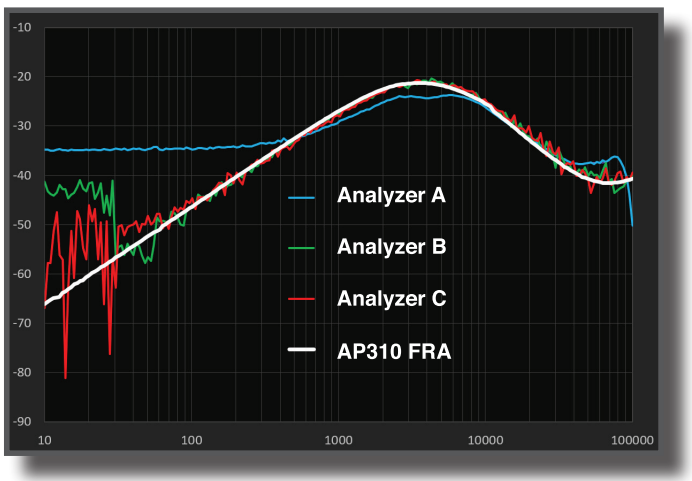

Full Calibration and Certification

Z540-1 Military calibration and certification with full data
NIST Calibration and certification with full data
2-year warranty